Contribution from the Istituto di Chimica Generale ed Inorganica, Università, Laboratorio CNR, Florence, Italy

Low-Temperature Crystal Structure and Electron Spin Resonance Spectra of Bis(isothiocyanato)[*N*-(2-(diphenylphosphino)ethyl)-*N'*,*N'*-diethylethylenediamine]cobalt(II), a Five-Coordinate Complex Exhibiting Spin Equilibrium

D. GATTESCHI, C. A. GHILARDI, A. ORLANDINI, and L. SACCONI*

Received March 30, 1978

The problem of the temperature-dependent spin equilibrium exhibited by the five-coordinated $[Co(NCS)_2(nnp)]$ (nnp = $(C_2H_5)_2NCH_2CH_2NHCH_2CH_2P(C_6H_5)_2$) complex is reexamined in the light of variable-temperature ESR measurements and an X-ray diffraction study at 120 K. The crystals are triclinic, space group $P\bar{1}$, with the following cell dimensions: a = 15.669 (10) Å, b = 8.813 (6) Å, c = 9.368 (7) Å, α = 111.9 (1)°, β = 93.8 (1)°, γ = 91.3 (1)°, Z = 2. The structure was refined by full-matrix least-squares methods to the final conventional R factor 0.076. The variable-temperature ESR spectra, in accord with previous IR data, suggest the existence of a temperature-dependent population of two geometrically different forms in two different spin states. The low-temperature X-ray diffraction data show significant variations of the structural parameters of the complex as compared with those of room temperature previously reported. The high-spin–low-spin interconversion is accompanied by an increased distortion of the structure toward an elongated square pyramid. The room-temperature thermal parameters are reexamined and discussed.

Introduction

In the last years some five-coordinate cobalt(II) and nickel(II) complexes have been reported to exhibit temperature-dependent spin transitions.[1-4] The spin state in this class of complexes, as well as the position of the crossover point, has been correlated to both the electronegativity and the nucleophilicity of the donor atoms.[5] A particularly interesting case is that of the isothiocyanate complex of cobalt(II) with the tridentate ligand *N*-(2-(diphenylphosphino)ethyl)-*N'*,*N'*-diethylethylenediamine (nnp).[4] The value of the magnetic moment of this complex has been found to vary smoothly with the temperature from 2.16 μ_B at 79 K, corresponding to an essentially low-spin state, up to 4.32 μ_B at 418 K, indicative of high-spin cobalt(II). Also the electronic spectra were found to vary correspondingly in the same range of temperature.

The infrared spectra recorded between 77 and 400 K suggested the existence of an equilibrium between molecules with different structures,[6,7] but the X-ray structural data at room temperature were interpreted as indicative of the existence of a molecule intermediate between the limit high- and low-spin forms.[8]

Since one of the much-debated problems in the study of spin equilibria[9-13] is still that of the possible existence of an intermediate spin state,[14] as opposed to a mixture of two different species, one high and the other low spin, we resolved to gain new experimental data for the complex $[Co(NCS)_2(nnp)]$ by recording polycrystalline powder ESR spectra in the range 300–77 K and by collecting three-dimensional counter data at 120 K. We report here the results of these investigations.

Experimental Section

The crystal used for X-ray data collection had dimensions of 0.05 × 0.06 × 0.4 mm. The sample was mounted so that its longest dimension was approximately parallel to the ϕ axis of the four-circle automatic Philips PW 1100 diffractometer. The low-temperature data were collected by using a Leybold-Heraeus cryostat, the cooling being effected by blowing a cold nitrogen gas stream onto the sample.

The space group[8] does not change on cooling, the new cell constants being a = 15.669 (10) Å, b = 8.813 (6) Å, c = 9.368 (7) Å, α = 111.9 (1)°, β = 93.8 (1)°, and γ = 91.3 (1)°. The volume goes from 1218.58 Å^3 at room temperature to 1196.20 Å^3 at 120 K. Data collection was carried out using Mo Kα (λ 0.7107 Å) radiation monochromatized with a graphite crystal. Reflections within $2\theta \leq 50°$ were collected using the ω–2θ scan technique with a scan range of 1.6° and a scan speed of 0.16°/s in 2θ. Stationary background measurements were taken before and after each scan for a time equal to half the scan time. Three standard reflections recorded every 60 min showed no significant variation in intensity during data collection. After correction for background, the intensities were assigned standard deviations calculated as described elsewhere[15] using the value of 0.05 for the instability factor p. A total of 2713 reflections having $I \geq 3\sigma(I)$ were considered observed.

Owing to the very irregular shape of the crystal, no absorption correction could be applied. The linear absorption coefficient μ(Mo Kα) was 9.73 cm^{-1}. The effect of anomalous dispersion for Co, S, and P atoms was considered in the calculation of F_c.[16] Scattering factors for nonhydrogen atoms were taken from ref 17 and those for hydrogen atoms from ref 18.

The refinement of the structure was undertaken using the final parameters of the room-temperature structure, the function minimized being $\sum w(|F_o| - |F_c|)^2$, where w is $1/\sigma^2(F_o)$. After an isotropic cycle on all atoms, a series of full-matrix isotropic–anisotropic cycles, with anisotropic thermal parameters associated with the heavier atoms, was performed. Since an unusual high temperature factor was observed for the terminal carbon of an ethylenic chain, a difference Fourier syntheses was calculated at this stage. It showed that this carbon is disordered over two half-populated sites. The refinement carried out using a population parameter of $^1/_2$ associated with each of the two positions led easily to convergence. It is worth noting that this carbon atom in the room-temperature structure has the highest thermal parameter of the molecule. Hydrogen atoms were introduced in their geometrical positions with C–H = 0.95 Å. The final R and R_w values are respectively 0.076 and 0.098, R_w being defined as $[\sum w(|F_o| - |F_c|)^2/\sum w|F_o|^2]^{1/2}$. The standard deviation of an observation of unit weight is 1.82. Tables I and II show the final parameters with their estimated standard deviations.

The ESR spectra were recorded with a Varian E-9 spectrometer, equipped with X-band (9 GHz) and variable-temperature accessories.

Results and Discussion

In Table III the bond distances and angles for the coordination polyhedra of $[Co(NCS)_2(nnp)]$ at 120 and 298 K are shown. For comparison purposes bond distances and angles of the closely related complex $[Co(NCS)_2(Me(nnp))]$[8] are also reported. This compound which contains as a ligand the *N*-methyl derivative of nnp, $(C_2H_5)_2NCH_2CH_2N(CH_3)CH_2CH_2P(C_6H_5)_2$, has a magnetic moment of 4.47 μ_B independent of temperature. Figures 1 and 2 show perspective views of the $[Co(NCS)_2(nnp)]$ complex at the two temperatures. Table IV gives other bond distances and angles of the same compound at 120 K.

The $[Co(NCS)_2(nnp)]$ chromophore possesses both at 120 and at 298 K a very low symmetry with a geometry intermediate between that of a square pyramid and that of a trigonal bipyramid. Significant variations in some bond distances and angles are observed on passing from room to low temperature. Thus the N(3)–Co–P angle increases by 10°, passing from 148 to 158°, and the Co–P and Co–N(4) dis-

0020-1669/78/1317-3023$01.00/0

Table I. Positional Parameters (×10⁴) and Isotropic Temperature Factors with Estimated Standard Deviations in Parentheses

atom	*x/a*	*y/b*	*z/c*	10^3U, Å²
Co	2600 (1)	1241 (1)	1287 (1)	*a*
S(1)	4477 (1)	−3206 (2)	−1012 (2)	*a*
S(2)	1130 (1)	−3136 (2)	1899 (3)	*a*
P	3063 (1)	2321 (2)	3788 (2)	*a*
N(1)	3562 (4)	−374 (8)	360 (7)	*a*
N(2)	1899 (4)	−431 (8)	1503 (7)	*a*
N(3)	1953 (4)	1097 (7)	−778 (7)	*a*
N(4)	3302 (4)	3065 (7)	1114 (7)	*a*
C(1)	3935 (4)	−1538 (9)	−230 (8)	*a*
C(2)	1566 (4)	−1579 (9)	1640 (8)	*a*
C(3)	2550 (5)	1975 (9)	−1423 (9)	28 (2)
C(4)	2926 (5)	3511 (9)	−185 (9)	28 (2)
C(5)	3495 (5)	4518 (9)	2557 (9)	28 (2)
C(6)	3835 (5)	3921 (9)	3824 (9)	29 (2)
C(7)	3599 (4)	1235 (8)	4890 (8)	25 (2)
C(8)	3322 (5)	−382 (9)	4594 (9)	34 (2)
C(9)	3714 (5)	−1153 (10)	5533 (10)	40 (2)
C(10)	4354 (5)	−371 (10)	6638 (9)	38 (2)
C(11)	4633 (5)	1213 (10)	6916 (10)	40 (2)
C(12)	4250 (5)	2004 (9)	6019 (9)	34 (2)
C(13)	2261 (5)	3388 (9)	5105 (9)	28 (2)
C(14)	1415 (6)	2712 (11)	4807 (11)	51 (2)
C(15)	811 (7)	3381 (13)	5866 (12)	60 (3)
C(16)	1040 (6)	4697 (11)	7204 (11)	47 (2)
C(17)	1874 (5)	5355 (10)	7510 (9)	35 (2)
C(18)	2480 (5)	4688 (9)	6453 (9)	26 (2)
C(19)	1140 (6)	2024 (11)	−408 (10)	45 (2)
C(201)	958 (11)	2725 (22)	1143 (22)	45 (4)
C(202)	460 (10)	1386 (20)	212 (19)	39 (4)
C(21)	1781 (5)	−605 (10)	−1883 (10)	39 (2)
C(22)	1338 (7)	−823 (13)	−3465 (12)	60 (3)

[a] These atoms were refined anisotropically.

Table II. Anisotropic Thermal[a] Parameters (×10⁴) with Their Estimated Standard Deviations in Parentheses

atom	U_{11}	U_{22}	U_{33}	U_{12}	U_{13}	U_{23}
Co	212 (5)	311 (6)	311 (6)	35 (4)	55 (4)	243 (5)
S(1)	255 (10)	265 (10)	424 (12)	21 (8)	48 (9)	142 (9)
S(2)	440 (13)	318 (12)	528 (14)	−75 (10)	144 (11)	205 (11)
P	221 (10)	237 (10)	278 (11)	−13 (8)	−16 (8)	150 (9)
N(1)	284 (34)	327 (36)	371 (38)	97 (30)	63 (30)	214 (32)
N(2)	297 (35)	337 (37)	389 (39)	−34 (29)	50 (29)	212 (33)
N(3)	218 (31)	303 (34)	407 (37)	9 (25)	49 (28)	233 (30)
N(4)	233 (31)	249 (32)	335 (36)	−5 (25)	55 (27)	185 (29)
C(1)	231 (40)	329 (43)	357 (43)	−28 (34)	9 (33)	259 (37)
C(2)	230 (38)	336 (43)	282 (41)	24 (32)	73 (32)	139 (36)

[a] The form of the anisotropic thermal factor is $\exp[-2\pi^2(U_{11}h^2a^{*2} + U_{22}k^2b^{*2} + U_{33}l^2c^{*2} + 2U_{12}hka^*b^* + 2U_{13}hla^*c^* + 2U_{23}klb^*c^*)]$.

Table III. Bond Lengths (Å) and Angles (deg) with Estimated Standard Deviations in the Coordination Polyhedra

	[Co(NCS)₂(nnp)]		[Co(NCS)₂(Me(nnp))]
	120 K	298 K	
Co-P	2.237 (2)	2.32 (1)	2.40 (1)
Co-N(1)	2.097 (6)	2.04 (1)	1.97 (1)
Co-N(2)	1.897 (7)	1.92 (2)	2.02 (1)
Co-N(3)	2.083 (7)	2.07 (1)	2.14 (1)
Co-N(4)	1.990 (7)	2.10 (1)	2.36 (1)
P-Co-N(1)	101.6 (2)	105.1 (4)	110.3 (3)
P-Co-N(2)	94.1 (2)	96.5 (4)	101.1 (3)
P-Co-N(3)	158.0 (2)	148.0 (3)	111.0 (3)
P-Co-N(4)	85.0 (2)	82.0 (3)	79.6 (3)
N(1)-Co-N(2)	92.5 (3)	95.3 (6)	98.1 (5)
N(1)-Co-N(3)	98.2 (2)	102.6 (5)	132.7 (4)
N(1)-Co-N(4)	89.9 (3)	89.6 (5)	86.0 (4)
N(2)-Co-N(3)	94.5 (3)	96.6 (5)	95.8 (4)
N(2)-Co-N(4)	177.6 (3)	175.1 (5)	175.3 (5)
N(3)-Co-N(4)	85.6 (3)	82.4 (4)	79.7 (4)

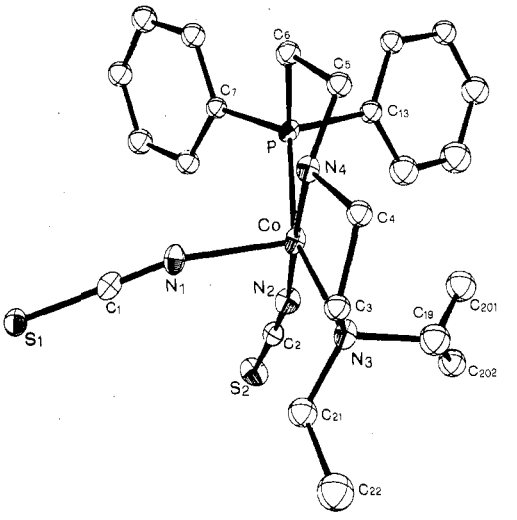

Figure 1. Perspective view of the [Co(NCS)₂(nnp)] complex at 120 K (30% probability ellipsoids).

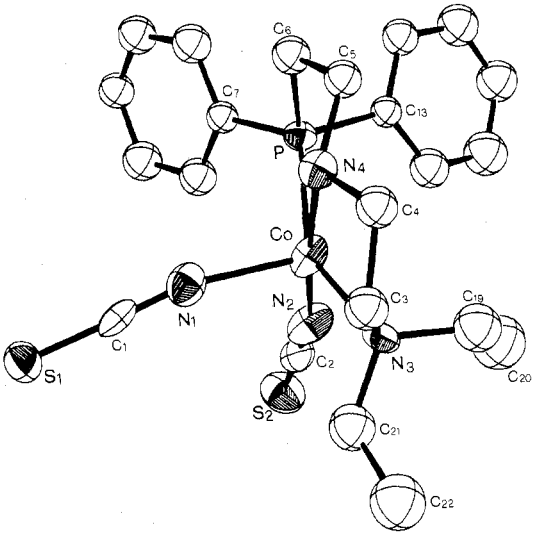

Figure 2. Perspective view of the [Co(NCS)₂(nnp)] complex at 298 K (30% probability ellipsoids).

Table IV. Selected Bond Lengths (Å) and Angles (deg) with Estimated Standard Deviations

Bond Lengths			
S(1)-C(1)	1.660 (7)	N(3)-C(21)	1.48 (1)
S(2)-C(2)	1.624 (9)	N(4)-C(4)	1.50 (1)
P-C(6)	1.827 (8)	N(4)-C(5)	1.48 (1)
P-C(7)	1.828 (9)	C(3)-C(4)	1.49 (1)
P-C(13)	1.839 (7)	C(5)-C(6)	1.54 (1)
N(1)-C(1)	1.16 (1)	C(19)-C(201)	1.40 (2)
N(2)-C(2)	1.18 (1)	C(19)-C(202)	1.45 (2)
N(3)-C(3)	1.49 (1)	C(21)-C(22)	1.54 (1)
N(3)-C(19)	1.52 (1)		
Bond Angles			
Co-P-C(6)	101.5 (3)	Co-N(4)-C(5)	116.2 (5)
Co-P-C(7)	126.0 (2)	C(4)-N(4)-C(5)	112.3 (6)
Co-P-C(13)	115.3 (2)	S(1)-C(1)-N(1)	178.0 (8)
C(6)-P-C(7)	105.9 (3)	S(2)-C(2)-N(2)	177.6 (7)
C(6)-P-C(13)	105.5 (3)	N(3)-C(3)-C(4)	110.5 (6)
C(7)-P-C(13)	100.8 (4)	N(4)-C(4)-C(3)	107.6 (7)
Co-N(1)-C(1)	163.8 (6)	N(4)-C(5)-C(6)	108.1 (6)
Co-N(2)-C(2)	170.8 (6)	P-C(6)-C(5)	106.0 (5)
Co-N(3)-C(3)	104.0 (4)	P-C(7)-C(8)	118.6 (5)
Co-N(3)-C(19)	108.3 (5)	P-C(7)-C(12)	120.8 (6)
Co-N(3)-C(21)	112.9 (6)	P-C(13)-C(14)	118.4 (5)
C(3)-N(3)-C(19)	109.4 (7)	P-C(13)-C(18)	122.0 (6)
C(3)-N(3)-C(21)	109.6 (6)	N(3)-C(19)-C(201)	118.1 (1.1)
C(19)-N(3)-C(21)	112.3 (6)	N(3)-C(19)-C(202)	119.2 (1.0)
Co-N(4)-C(4)	110.1 (4)	N(3)-C(21)-C(22)	116.4 (8)

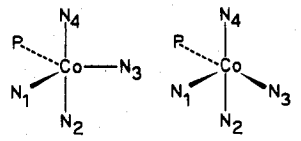

Figure 3. Limit geometries for high- and low-spin forms of the cobalt complex.

tances become shorter by 0.08 and 0.11 Å, respectively, on cooling, whereas the Co–N(1) distance increases by 0.06 Å. The magnetic moment of $[Co(NCS)_2(nnp)]$ at 120 K, 2.20 μ_B, is very close to the lowest value observed, 2.16 μ_B,[4] so that the low-temperature X-ray diffraction data can be considered to provide the structural parameters for the complex in the low-spin state. On the other hand, the magnetic moment of 3.6 μ_B at 298 K suggests that at room temperature the system is about halfway between the high- and the low-spin state. The structural parameters of the complex $[Co(NCS)_2(nnp)]$ in the high-spin state are not available, but a reasonable guess of them can be made by considering those of the complex $[Co(NCS)_2(Me(nnp))]$.[8] In this compound which was described as essentially trigonal bipyramidal, the N(3)–Co–P angle is 111°. It is therefore apparent that the high-spin to low-spin interconversion is accompanied by an increase in distortion toward an elongated square pyramid having N(1) at the apex (Figure 3).

The data of Table III show that the N(3)–Co–P angle and the Co–P, Co–N(4), and Co–N(1) bond distances vary monotonically on passing from low-temperature $[Co(NCS)_2(nnp)]$ through room-temperature $[Co(NCS)_2(nnp)]$ to $[Co(NCS)_2(Me(nnp))]$.

The other distances in the coordination polyhedron of $[Co(NCS)_2(nnp)]$ do not change significantly on cooling. It is worth noting that the observed shortening of the Co–N(4) distance at low temperature is in accordance with the lowering of the N(4)–H stretching frequency observed in the IR spectra when the temperature is lowered.[6]

The geometrical variations observed for $[Co(NCS)_2(nnp)]$ are quite large if compared with those reported for other octahedral iron(II) complexes exibiting spin equilibria.[19,20] The larger fluxionality of the five-coordinate stereochemistries as compared to the octahedral ones may be responsible for this behavior.

It has been pointed out in previous studies[21,22] that in the five-coordinated cobalt(II) complexes the low-spin form is stabilized relative to the high-spin form by a distortion toward an elongated square pyramid. The shortening of the Co–P and Co–N(4) bond lengths determines a larger ligand field strength in the basal plane of the square pyramid while the lengthening of the Co–N(1) distance decreases the ligand field perpendicular to this plane. If the z axis is taken parallel to the Co–N(1) bond direction, the unpaired electron of the low-spin form must be placed in the z^2 orbital. This result was found also by angular overlap calculations, using the reported values for the e_λ parameters.[23]

The polycrystalline powder ESR spectra are typical of a spin doublet possessing axial symmetry.[24] The g values are $g_\parallel$ = 2.02 and $g_\perp$ = 2.32. No hyperfine structure was observed due to the fact that the paramagnetic centers are not diluted. The fields of absorption remain practically unchanged from room temperature to 77 K, while the intensities of the signals largely increase on cooling. These experimental data suggest that in every case the ESR absorptions are due to the low-spin molecule, the signals of the high-spin form being in every case too broad to be detected. The ESR spectra therefore indicate the existence of two different molecules for the high- and low-spin states. Therefore, as suggested also by the IR data,[6,7] the possibility of an intermediate spin state molecule must be ruled out. The rate of interconversion of the high- and low-spin forms must be slower than the inverse time scale of the ESR experiment, 10^{10} s^{-1}.

Table V. Root-Mean-Square Displacements (Å) of Principal Axes of Thermal Ellipsoids for the Atoms of the Coordination Polyhedra[a]

	axis 1	axis 2	axis 3
Co	0.104	0.144	0.201
	0.200	0.219	0.305
	0.201	0.218	0.222
P	0.129	0.144	0.179
	0.200	0.220	0.237
	0.194	0.220	0.224
N(1)	0.136	0.167	0.209
	0.233	0.263	0.300
	0.223	0.273	0.283
N(2)	0.138	0.185	0.206
	0.245	0.258	0.359
	0.214	0.249	0.259
N(3)	0.130	0.152	0.210
	0.178	0.224	0.269
	0.193	0.240	0.267
N(4)	0.117	0.158	0.190
	0.206	0.244	0.254
	0.202	0.235	0.259

[a] For each atom, the first line gives the root-mean-square displacements of $[Co(NCS)_2(nnp)]$ at 120 K, the second line those of $[Co(NCS)_2(nnp)]$ at 298 K, and the third line those of $[Co(NCS)_2(Me(nnp))]$.

The observed g values follow the pattern expected for an unpaired electron in an orbital which is mainly z^2 in nature,[25] in accordance with the energy level calculations above. The values compare well with those reported for low-spin $Co(NCS)(dpe)_2ClO_4$,[26] where dpe is 1,2-bis(diphenylphosphino)ethane.

If the observed g values are used to calculate the magnetic moment of the low-spin form, the value of 1.92 μ_B is obtained, which is sensibly lower than the lowest value of 2.16 μ_B observed at 120 K. This difference may be due to the neglect of TIP contributions and/or to the permanence of a small percentage of high-spin form even at low temperatures, as observed[27] and theoretically justified[28] for iron(II) complexes exhibiting spin equilibria.

Conclusion

Both the IR and the ESR data suggest that the spin equilibrium in the complex $[Co(NCS)_2(nnp)]$ is determined by a temperature-dependent population of quartet and doublet spin states which interconvert at a rate slower than 10^{10} s^{-1}. This conclusion demands that the room-temperature X-ray data, which were interpreted as indicative of the existence of only one molecule in an intermediate spin state,[8] be reexamined. The presence of two different molecules in equilibrium was ruled out on the basis of both the lack of disorder and the close similarity of the thermal motion of $[Co(NCS)_2(nnp)]$ with that of $[Co(NCS)_2(Me(nnp))]$, which is high spin. On the other hand, no absorption corrections could be applied to these complexes, so a meaningful analysis of the thermal parameters cannot be attempted. However, a qualitative comparison of the root-mean-square displacements as shown in Table V appears to be of interest. Leipoldt and Coppens[20] suggested that the thermal parameters for a spin equilibrium system are given by the relation

$$U_{ij}(\text{new}) = U_{ij}(\text{old}) + x_0^2$$

where U_{ij}(old) are the thermal parameters of an atom in the absence of spin equilibrium, U_{ij}(new) are the thermal parameters for an equimolar mixture of high- and low-spin forms, and $2x_0$ is the difference in the position of the donor atoms

in the high- and the low-spin forms. In the present case, x_0 can be as large as 0.2 Å for the P and N(3) donor atoms taking into account bond-distance and -angle variations. This effect does not appear evident from the data of Table V. The ratio of the values at room and low temperature appears to be normal. Also the root-mean-square displacements for the two room-temperature structures appear to be quite similar. The only exception is that of the parameters for the Co and N(2) atoms which appear to be larger for the intermediate-spin complex. However, these differences can be hardly rationalized as the Co–N(2) bond distance does not change on cooling.

Finally, although the interpretation of the X-ray diffraction data still leaves some problems open, IR and ESR data are in favor of the hypothesis of a disordered spin state.

Registry No. $Co(NCS)_2(nnp)$, 29993-37-1.

Supplementary Material Available: A listing of calculated and observed structure factor amplitudes (14 pages). Ordering information is given on any current masthead page.

References and Notes

(1) W. S. J. Kelly, G. H. Ford, and S. M. Nelson, *J. Chem. Soc. A*, 388 (1971).
(2) W. V. Dahlhoff and S. M. Nelson, *J. Chem. Soc. A*, 2184 (1971).
(3) L. G. Marzilli and P. A. Marzilli, *Inorg. Chem.*, **11**, 457 (1972).
(4) R. Morassi, F. Mani, and L. Sacconi, *Inorg. Chem.*, **12**, 1246 (1973).
(5) L. Sacconi, *J. Chem. Soc. A*, 248 (1970).
(6) R. Morassi and L. Sacconi, *J. Am. Chem. Soc.*, **92**, 5241 (1970).
(7) L. Sacconi and J. R. Ferraro, *Inorg. Chim. Acta*, **9**, 49 (1974).
(8) A. Bianchi Orlandini, C. Calabresi, C. A. Ghilardi, P. L. Orioli, and L. Sacconi, *J. Chem. Soc., Dalton Trans.*, 1383 (1973).
(9) E. König, *Coord. Chem. Rev.*, **3**, 471 (1968).
(10) L. Sacconi, *Pure Appl. Chem.*, **17**, 95 (1968).
(11) H. A. Goodwin, *Coord. Chem. Rev.*, **18**, 293 (1976).
(12) R. J. Butcher, J. R. Ferraro, and E. Sinn, *Inorg. Chem.*, **15**, 2077 (1976).
(13) G. R. Hall and D. N. Hendrickson, *Inorg. Chem.*, **15**, 607 (1976).
(14) G. Harris, *Theor. Chim. Acta*, **10**, 119, 155 (1968).
(15) P. W. R. Corfield, R. J. Doedens, and J. A. Ibers, *Inorg. Chem.*, **6**, 197 (1976).
(16) D. T. Cromer, *Acta Crystallogr.*, **18**, 17 (1965).
(17) D. T. Cromer and J. T. Waber, *Acta Crystallogr.*, **18**, 104 (1965).
(18) R. F. Stewart, E. R. Davidson, and W. T. Simpson, *J. Chem. Phys.*, **42**, 3175 (1965).
(19) E. König and K. J. Watson, *Chem. Phys. Lett.*, **6**, 457 (1970).
(20) J. G. Leipoldt and P. Coppens, *Inorg. Chem.*, **12**, 2269 (1973).
(21) L. Sacconi, *Coord. Chem. Rev.*, **8**, 351 (1972).
(22) R. Morassi, I. Bertini, and L. Sacconi, *Coord. Chem. Rev.*, **11**, 343 (1973).
(23) I. Bertini, D. Gatteschi, and A. Scozzafava, *Inorg. Chem.*, **14**, 1639 (1975).
(24) B. R. McGarvey, *Transition Met. Chem.*, **3**, 90 (1966).
(25) J. S. Griffith, *Discuss. Faraday Soc.*, **26**, 81 (1958).
(26) Y. Nishida and H. Shimohori, *Bull. Chem. Soc. Jpn.*, **46**, 2406 (1973).
(27) E. König, G. Ritter, and H. A. Goodwin, *Chem. Phys.*, **1**, 17 (1973).
(28) R. A. Bari and J. Sivardiere, *Phys. Rev. B*, **5**, 4466 (1972).

Contribution from the Department of Chemistry, Northwestern University, Evanston, Illinois 60201, and the Inorganic Chemistry Section, National Bureau of Standards, Washington, D.C. 20234

Iridium(I) and Rhodium(I) Complexes of Benzotriazole. Structure of Bis(triphenylphosphine)carbonyl(benzotriazenido)iridium(I)

LEO D. BROWN,[1a] JAMES A. IBERS,*[1a] and ALLEN R. SIEDLE*[1b]

Received March 24, 1978

Thallium benzotriazenide has been prepared from benzotriazole, thallium(I) acetate, and triethylamine in ethanol. The compound serves as a convenient starting material for the synthesis of organometallic benzotriazenides. It reacts with $[Ir(CO)(acetone)(PPh_3)_2][PF_6]$ to yield the tetramer $[Ir(BTA)(CO)(PPh_3)]_4$, where Ph = phenyl and BTA = benzotriazenido. A similar reaction with $RhCl(CO)(PPh_3)_2$ yields the hexamer $[Rh(BTA)(CO)(PPh_3)]_6$. Direct reaction of Tl(BTA) with $IrCl(CO)(PPh_3)_2$ yields $Ir(BTA)_2(CO)(PPh_3)Tl{\cdot}C_6H_6$. A methanol solution of this material rapidly changes color from violet to yellow and from this solution the compound $Ir(BTA)(CO)(PPh_3)_2$ is obtained. On the basis of an X-ray crystal structure, the Ir atom in $Ir(BTA)(CO)(PPh_3)_2$ is coordinated by trans P atoms, the CO ligand, and the BTA ligand in nearly a square-planar arrangement. Despite the symmetric nature of the N_3 portion of the BTA ligand, the ligand is coordinated to the Ir atom through atom N(1). The ligand makes an angle of approximately 78° with the $Ir(CO)P_2$ plane. The compound crystallizes with four molecules in space group C_{2h}^5-$P2_1/n$ of the monoclinic system in a cell of dimensions a = 13.508 (3) Å, b = 20.225 (4) Å, c = 13.372 (3) Å, and β = 103.36 (1)°. The structure has been refined by full-matrix least-squares methods to a final R index of 0.035 for 199 variables, based on 6321 observations.

Introduction

Structure and bonding in transition-metal triazenido complexes have attracted much interest in recent years. The triazenido ligand may function as a bridging group between two metal centers (I), a bidentate, three-electron donor (II), or a monodentate, one-electron donor (III). Reported

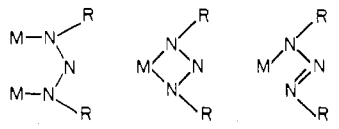

I II III

structures of triazenido complexes have been summarized.[2,3] The conjugate base of benzotriazole, **1**, is a particularly interesting triazenido ligand **2**, because of the conformational rigidity imposed by the fused benzene ring and the anticipated delocalization energy associated with the cyclic $C_2N_3^-$ system **2**. This paper reports the synthesis of rhodium(I) and iridium(I) derivatives of **2** and the structure of bis(triphenylphosphine)carbonyl(benzotriazenido)iridium(I), $Ir(BTA)(CO)(PPh_3)_2$, where BTA = benzotriazenido.

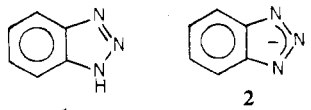

1 2

Experimental Section

All analyses were performed by Schwarzkopf Microanalytical Laboratory, Woodside, N.Y. The method used for the analysis of Ir is that of Ayres and Quick.[4] Molecular weights were determined by vapor pressure osmometry.

Syntheses. Thallium Benzotriazenide [Tl(BTA)]. Thallium(I) acetate, 5.26 g (20 mmol), was dissolved in 100 mL of hot absolute ethanol. The solution was filtered and to it was added 2.24 g (20 mmol) of benzotriazole and 20 mmol of triethylamine in 15 mL of absolute ethanol. After the solution was cooled for 2 h in an ice bath, the thin flakes of thallium benzotriazenide were collected on a filter, washed with cold ethanol, and vacuum dried; yield 4.1 g (63%). The product is sufficiently pure at this point for synthetic purposes. An analytical sample was obtained as blades from hot water. Anal. Calcd for $C_6H_4N_3Tl$: C, 22.35; H, 1.24; N, 13.04; Tl, 63.35. Found: C, 22.28; H, 1.22; N, 13.44; Tl, 63.50. IR (Nujol): 1475 (m), 1270

0020-1669/78/1317-3026$01.00/0